IMPLICATIONS OF CARBONATE PETROLOGY AND GEOCHEMISTRY FOR THE ORIGIN OF COAL BALLS FROM THE KALO FORMATION (MOSCOVIAN, PENNSYLVANIAN) OF IOWA

A Thesis

by

COURTNEY PAGE JONES

Submitted to the Office of Graduate Studies of
Texas A&M University
in partial fulfillment of the requirements for the degree of

MASTER OF SCIENCE

August 2012

Major Subject: Geology

IMPLICATIONS OF CARBONATE PETROLOGY AND GEOCHEMISTRY FOR THE ORIGIN OF COAL BALLS FROM THE KALO FORMATION (MOSCOVIAN, PENNSYLVANIAN) OF IOWA

A Thesis

by

COURTNEY PAGE JONES

Submitted to the Office of Graduate Studies of
Texas A&M University
in partial fulfillment of the requirements for the degree of

MASTER OF SCIENCE

Approved by:

Chair of Committee,	Anne Raymond
Committee Members,	Renald Guilemette
	Matthew Schmidt
	Mitchell Malone
	Michael Tice
Head of Department,	Rick Giardino

August 2012

Major Subject: Geology

ABSTRACT

Implications of Carbonate Petrology and Geochemistry for the Origin of Coal Balls from the Kalo Formation (Moscovian, Pennsylvanian) of Iowa. (August 2012)

Courtney Page Jones, B.S., Texas A&M University

Chair of Advisory Committee: Dr. Anne Raymond

Coal balls are carbonate concretions formed in peat during the Pennsylvanian and early Permian. Microprobe and microscope analysis reveal that polycrystals of high-Mg calcite (HMC), which are also high in Sr, are the earliest calcium carbonate to form in the Williamson No. 3 coal balls from the Kalo formation in Iowa. This HMC has early diagenetic rims of ferroan and non-ferroan low-Mg calcite (LMC) suggesting diagenesis in meteoric water. The combination of HMC followed by LMC suggests the earliest coal ball carbonate formed in a hydrologically dynamic environment, where saltwater influx into the mire was followed by a return to meteoric pore water. Subsequent generations of carbonate are ferroan and non-ferroan LMC and appear to result from diagenesis of the original HMC fabric with LMC rims. HMC polycrystals from coal balls are among the first abiotic HMC to be reported from the mid-Pennsylvanian; coal balls may be a good source of Pennsylvanian HMC. Coal balls that formed in porous peat (i.e. wood and surficial leaf mats) commonly have abundant radiating arrays of HMC polycrystals.

Coal balls that formed in matrix-rich, low porosity peats consist primarily of permineralizing anhedral calcite, which is ferroan LMC. The link between the HMC and porous permeable peat is supported by the distribution of HMC and ferroan LMC in plant cells. Wood cells, which have porous walls, are filled with HMC; fiber cells, which have impermeable walls, are filled with ferroan LMC. This study demonstrates a link between pore volume, porosity, plant cell type, and carbonate fabric.

ACKNOWLEGEMENTS

This paper owes much to discussions with S. H. Costanza, J. Newman, W. C. Parker, T. L. Phillips, M. Pope, A. C. Scott, M. Tice, and E. L. Zodrow as well as with the late W. Ahr. We gratefully acknowledge the support of Southwestern Energy and AAPG grants-in-aid granted to C.P. Jones.

TABLE OF CONTENTS

LIST OF FIGURES

LIST OF TABLES

1. INTRODUCTION

Coal balls, carbonate concretions that formed in ancient peat, are spectacular examples of carbonate and pyrite permineralization of land plants. They contain a highly diverse assortment of land plants (lycopsids, sphenopsids, ferns, seed-ferns and cordaites) and a wide range of plant organs, including leaves, stems, roots, cones, sporangia and seeds. Recent studies of coal-ball petrology have focused on the specificity of land-plant permineralization and the role of plant organs and cell walls in carbonate and pyrite permineralization as well as silicification (Zodrow and Cleal, 1999; Zodrow et al., 2002; Boyce et al., 2010; Raymond et al., 2012). Coal balls from the Williamson No. 3 Mine (Kalo Formation) in south-central Iowa preserve a decomposition gradient in which the availability of pore space can be linked to both the taxonomic composition of the peat and the degree of decomposition. Cordaitean peat from the Williamson No. 3 Mine provides an ideal opportunity to investigate how pore size and connectivity influence the precipitation of pyrite and carbonate minerals during coal ball formation.

Many have studied the origin, carbonate petrology, geochemistry, and stable isotope composition of coal balls (Stopes and Watson, 1908; Mamay and Yochelson, 1962; Brownlee, 1973; Rao, 1979; Anderson et al., 1981; DeMaris et al., 1983; DeMaris, 2000; Scott and Rex, 1985; Scott et al., 1996; Zodrow et al., 1996; Zodrow and Cleal,

---

This thesis follows the style of *Palaios.*

1999; Zodrow et al., 2004; Boyce et al., 2010). However, few have considered the paragenetic sequence of coal-ball carbonate in detail. Because the paragenetic sequence of most coal ball deposits has not been fully interpreted, there is no consensus on how coal balls form, despite the large amount of research. There are three major challenges in forming an overarching theory of coal ball formation 1) Coal balls have been found in 65 Upper Carboniferous coal seams from over 200 locations in 9 countries (Scott and Rex, 1985); 2) Coal balls contain a wide range of authigenic minerals including pyrite, HMC (high-magnesium calcite), LMC (low-magnesium calcite), dolomite, and siderite; and 3) Based on their stable isotopic signatures, coal balls have been interpreted as freshwater carbonates; however, diagenetic alteration may have reset the original isotopic signatures of coal-ball carbonates. Based on carbonate geochemistry and the paragenetic sequence of carbonate fabrics and pyrite, Raymond et al. (2012) suggested that the Kalo Formation coal balls formed in a hydrologically dynamic environment, such that the earliest calcite precipitated from marine water and was diagenetically altered by oxic and anoxic meteoric water.

Porosity and permeability may be important in the formation of coal balls (Scott et al., 1996; Raymond et al., 2001; Raymond et al., 2012). In modern and ancient peat, pore size is controlled by plant organ and decomposition state, which typically correlates with depth in the mire. Near the surface of the peat mire, plant tissues retain their original form and porosity. Interparticle porosity occurs between plant organs. Intraparticle porosity depends on the plant tissues present in the deposit and is related to cavities within plant organs (e.g. pith cavities, seed chambers, sporangial cavities, and

root aerenchyma) and to the presence of porous plant tissues (e.g. tracheids, which are water conducting cells that form open channels in stems, wood, and in the vascular bundles of leaves, seeds, and other organs).

As decomposition proceeds, the porosity and permeability of peat decreases (Boelter, 1969; Clymo, 1983; Levesque and Mathur, 1979). Microbial attack weakens or destroys the structural biomolecules of plants (lignin, hemicellulose and cellulose), causing the plant debris to soften and deform, decreasing interparticle porosity. Peat compaction caused by the continued deposition of plant debris on the mire surface also contributes to the loss of interparticle porosity. Fungal decomposition weakens tracheid walls, causing them to crumple and collapse, once again, decreasing intraparticle porosity.

Although the net effect of peat decomposition is the loss of porosity, taphonomic processes can create porosity and enhance permeability. Fungal decomposition by simultaneous decay fungi destroys tracheid walls (Rayner and Boddy, 1998), increasing intraparticle porosity and permeability. Fungal decomposition by selective decay fungi destroy the middle lamina, which is found between tracheids, creating narrow pore spaces in wood (Rayner and Boddy, 1998). Aerenchymatous roots growing down through the peat increase the porosity and permeability of peat (Scott et al., 1996; Raymond et al., 2001). Finally, invertebrate detritivores that tunnel in wood and leaves, or that burrow in peat can increase both inter- and intraparticle porosity of peat (Raymond, 2012).

In this paper we investigate the relationship between the pore size and permeability of peat, the distribution of pyrite, and the carbonate geochemistry, of cordaites-dominated coal balls from the Williamson No. 3 Mine in the Kalo Formation (mid-Muscovian, Pennsylvanian) of Iowa. We show that the distribution of carbonate fabrics is linked to the size and distribution of pore spaces in peat due to three processes: 1) formation of HMC polycrystals inside tracheids; in cavities formed by plant organs (seed cavities, empty sporangia, pith cavities of stems, among others), and in cavities created by plant decomposition; 2) permineralization of plant cell walls by LMC; and 3) preferential recrystallization of HMC polycrystals to permineralizing anhedral LMC during burial diagenesis.

2. MATERIALS AND METHODS

2.1 Materials

This study builds on taphonomic and petrographic studies of permineralized peat (coal balls) from the Williamson No. 3 Mine in Lucas County, Iowa, which was part of the Pennsylvanian Western Interior Basin (Raymond, Cutlip and Sweet, 2001; Raymond et al., 2012; Fig. 1). This mine exploited a single coal seam, which could have been either the Blackoak, or the Cliffland coal of the Kalo Formation (Raymond et al., 2010). The Kalo Formation is mid Moscovian in age, and the North American Atokan-Desmoinesian stage boundary lies within the formation, such that the older Blackoak coal is latest Atokan in age, and the younger Cliffland coal is earliest Desmoinesian in age (Fig. 2). Coal balls were collected from the Williamson No. 3 Mine between 1930 and 1950, and donated to the Botanical Museum of Harvard University by F. O. Thompson, as part of the Thompson – Darrah Collection. Initially, these coal balls were gathered by miners, and there is no record of the stratigraphic position of individual specimens within the coal seam.

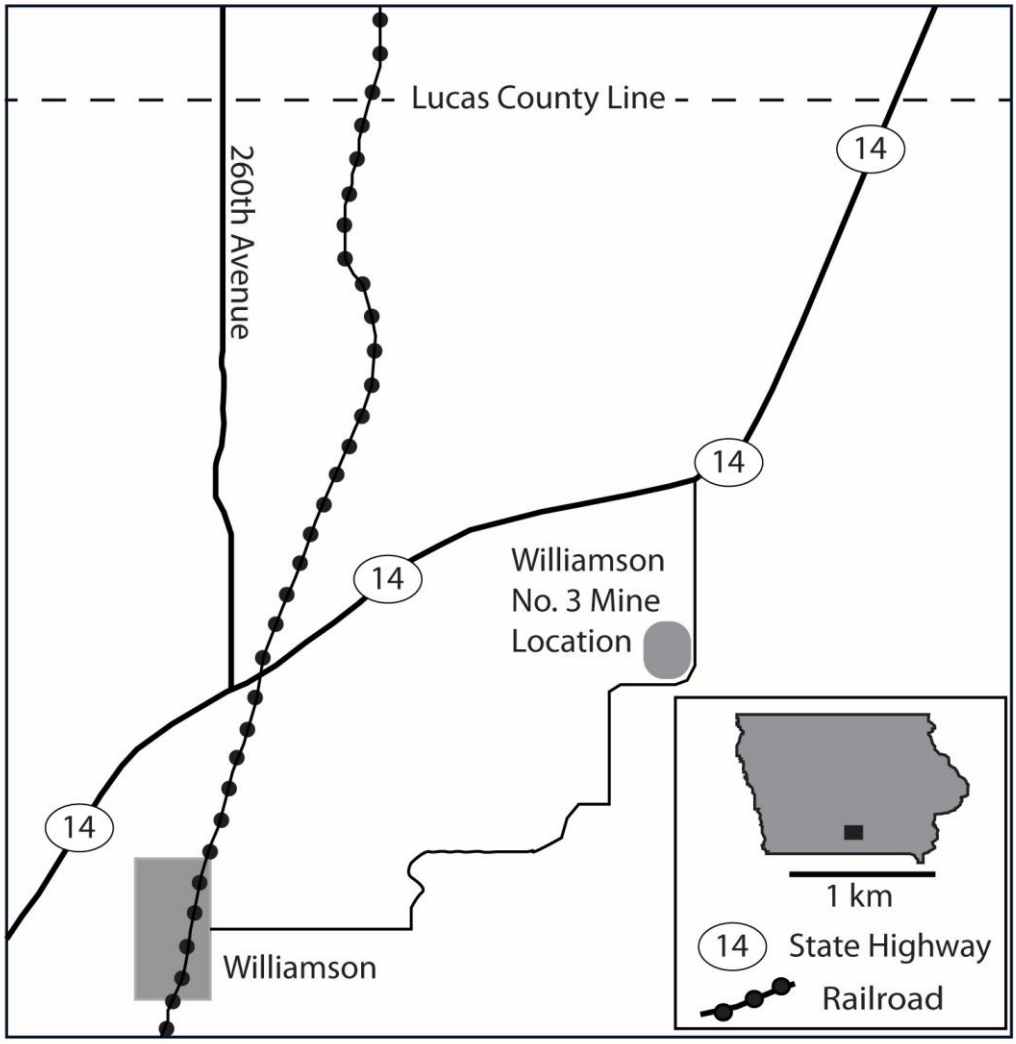

Figure 1. **Location Map of the Williamson No. 3 Mine.** Map of Iowa with the location of the reclaimed Williamson No. 3 Mine near Williamson, Iowa in Lucas County, adapted from Raymond et al. (2012).

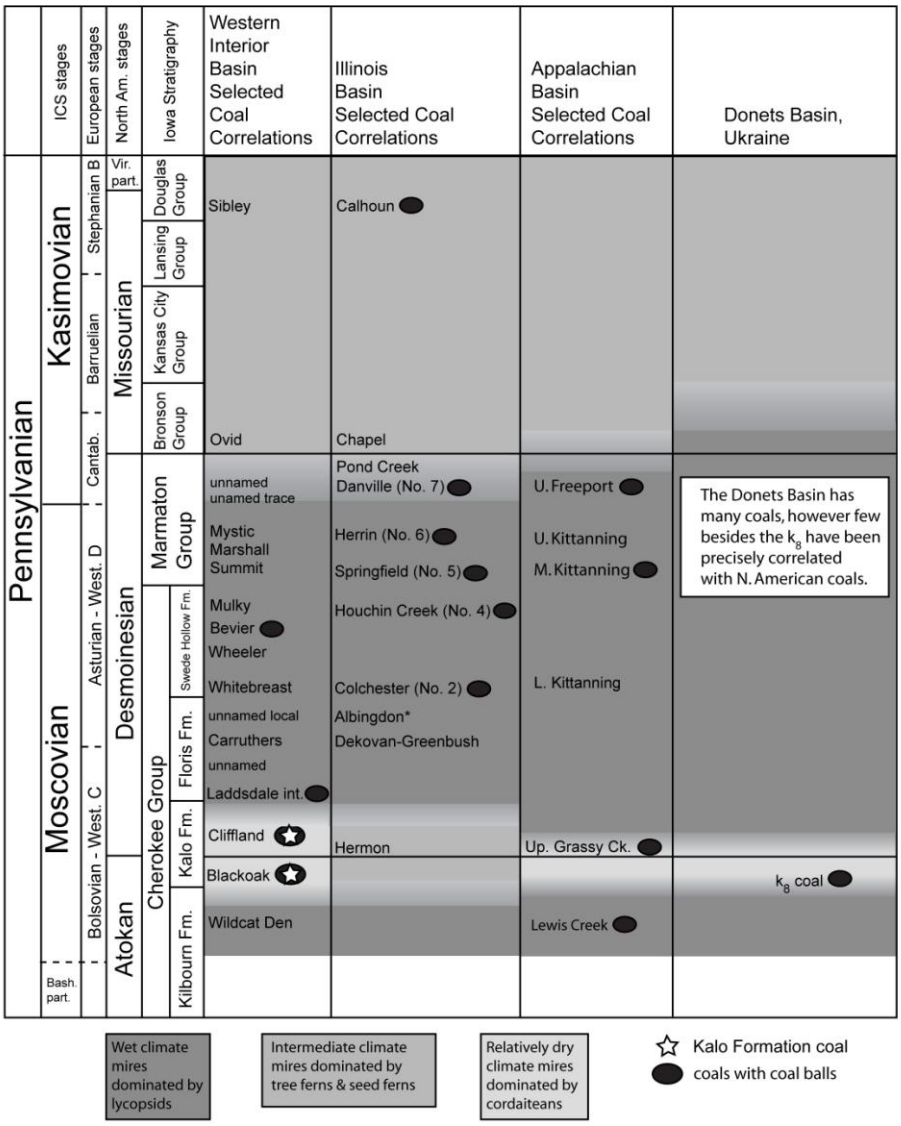

Figure 2. **Stratigraphic Column of Kalo Formation.** Stratigraphic position of the Williamson No. 3 coal ball deposit, which comes from one of the two Kalo Formation coals, either the Blackoak or the Cliffland coal, adapted from Raymond et al. (2012).

In order to investigate the carbonate petrology and geochemistry along a taphonomic gradient from pristine, well preserved peat to highly decomposed peat, we investigated the petrology and carbonate geochemistry of coal balls which contained: 1, cordaitean wood (2 coal balls, 5 polished thin sections); 2, pristine leaf mats invaded by cordaitean roots (2 coal balls, 4 polished thin sections); 3, decayed leaf mats in which individual leaves could still be discerned (2 coal balls, 3 polished thin sections); and 4, matrix rich peat consisting of peat matrix (organic particles with all dimensions ≤ 10 μm) roots and wood (1 coal ball, 1 polished thin-section; Fig. 3). The matrix rich peat sampled for this study consisted primarily of matrix. These four coal balls belong to three of the six types found in Williamson No. 3 coal balls based on the most common organic constituent in each: cordaitean wood; cordaitean leaf mat; cordaitean root; medullosan stem; medullosan root; and matrix (Raymond et al, 2001).

The peat types investigated for this study fall along a porosity gradient from porous, permeable leaf mat and wood peats to less porous and less permeable decayed leaf mat and matrix rich peat.

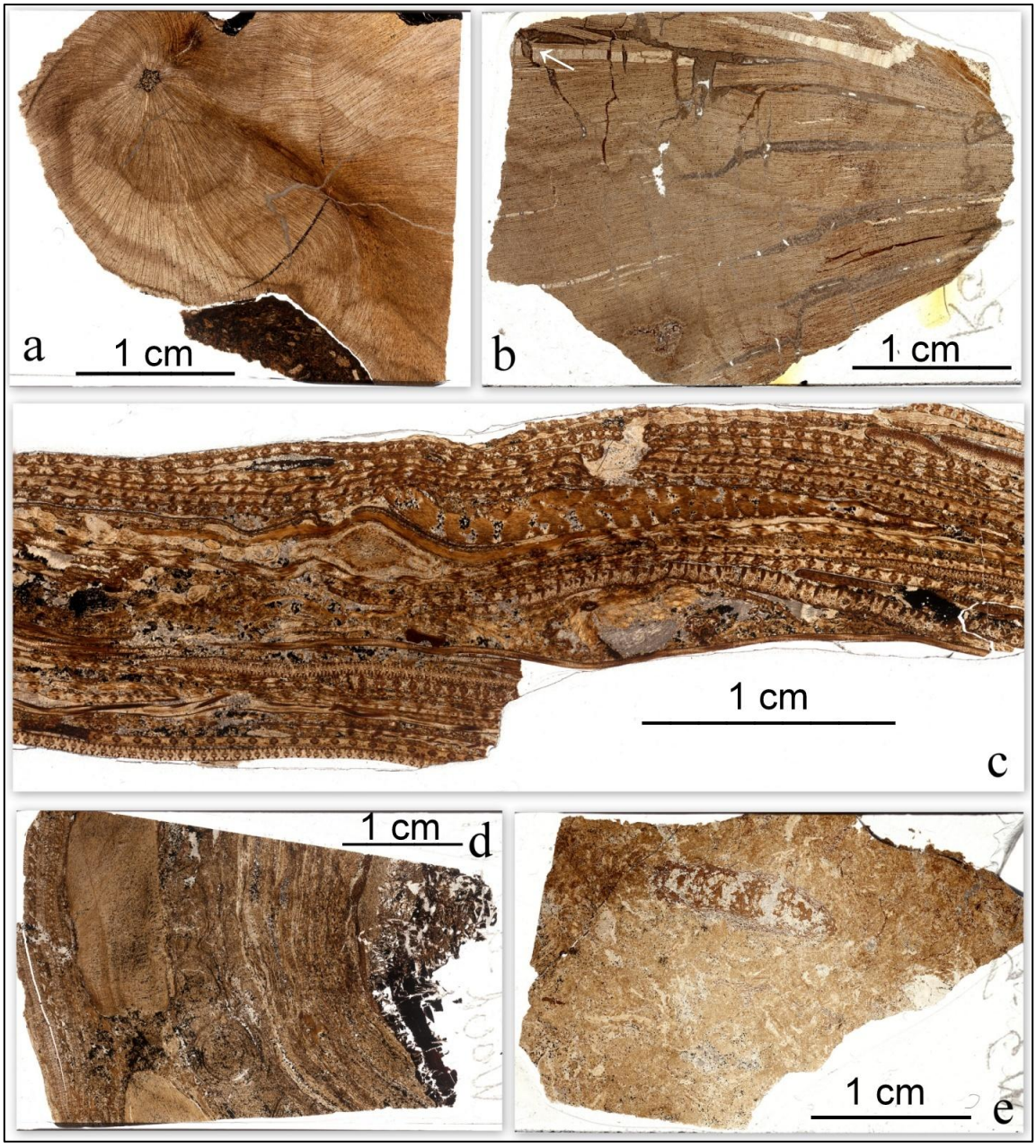

Figure 3. **Optical scans of study thin sections.** a) Pristine wood (W3-9dx); b) decayed wood (W3-3dx). Arrow indicates a vein of microcrystalline calcite B expanding as it crosses a vein of calcite 1; c) pristine leaf mat (W3-97-1); d) decayed leaf mat (Wood-97-19); e) matrix dominated (W3-5D).

2.2 Petrology and Geochemistry of Kalo Fm. Coal Balls

We used a Zeiss Axioplan 2 microscope with attached AxioCam HRc digital camera in orthoscopic mode for photomicroscopy and most petrology. We determined compositions of our samples using a Cameca SX50 electron microprobe equipped with four wavelength-dispersive X-ray spectrometers, a PGT energy-dispersive X-ray system and a panchromatic cathodoluminescence detector, housed in the Department of Geology and Geophysics at Texas A&M University. Standardizations and analyses were performed at an accelerating voltage of 15 kV, at a beam current of 10 or 50 nA, and at a beam diameter of 5 or 10 microns, depending on the sizes of the features available for analysis. Standardization and analysis conditions were matched for all analyses. Standardizations were carried out using well characterized carbonate mineral standards and silicates. Concentrations of the major elements (>10 wt %) are accurate to +/- 1-2 wt %. Statistical limits of detection for the minor and trace elements are as follows. The minor constituents MgCO3 and FeCO3 have detection limits of 0.05 and 0.10 mole %, respectively for the leaf peat analyses, and 0.01 and 0.03 mole %, respectively for all other analyses. The trace element Sr has a statistical limit of detection of 200 ppm by weight for all analyses. We include some major and minor element concentration data from a 1998 microprobe session, but have not used Sr data from this session due to the high statistical lower detection limit under the analytic conditions used at that time (900 ppm).

We augmented the 160 wavelength-dispersive compositional measurements with backscattered electron imaging (BSE). In BSE images pyrite is white or extremely light

grey; LMC is medium grey; HMC is dark grey; and dolomite is very dark grey. Void spaces, epoxy, and organic carbon walls are black. However unless otherwise noted, on BSE images used in this contribution, black represents organic carbon.

We used wavelength-dispersive elemental X-ray imaging to map the distribution of key elements. X-ray elemental distribution "maps" were obtained at 15 kV and 20 nA beam current in either beam or stage scanning mode, using the wavelength-dispersive X-ray spectrometers with one spectrometer each set on the Mg, Ca or Fe K alpha X-ray peak position. This yielded a separate image for each element showing where that element's X-rays were being emitted from the sample; a matching BSE image was also generated. For the 1mm map, the stage was rastered beneath the beam in a 512 by 512 point grid, with a grid spacing of 2 microns and a dwell time of approximately 15 milliseconds at each point. For the 2000x (46 μm) maps, the stage remained fixed and the beam was rastered in a 256 by 256 point grid, with a grid spacing of 0.24 microns and a total acquisition time of 300 seconds.

False-color X-ray maps were generated by combining the three binary thresholded Ca, Mg, and Fe images. In the resulting images, if only high Ca was detected, then low-Mg calcite was indicated, and a light green color was assigned to those pixels. When both high Ca and moderately high Mg were detected, then high-Mg calcite was indicated, and the color blue was used. When both high Ca and high Mg were detected, then non-ferroan dolomite was indicated, and the color green was used. When high Ca, high Mg and high Fe were all detected, then ferroan dolomite was indicated, and the color red was used. The presence of only high Fe corresponded to the

presence of pyrite, and the color brown was used. Finally, the color black was used to indicate the presence of organic carbon, epoxy cement or fractures. In the false-color images shown here, black indicates concentrations of organic carbon.

In addition to characterizing samples with the electron microprobe, we used a scanning electron microscope, the FEI Quanta 600 FE-SEM housed in the Microscopy and Imaging Center of Texas A&M University, to observe grain boundaries in decayed wood.

2.3 Paragenetic Sequence

Our paragenetic sequence for Williamson No. 3 coal balls builds on that of Raymond et al., (2012), and relies on cross-cutting relations in the wood and pristine leaf mat samples (Fig. 3a-c). Both these samples contain a range of carbonate fabrics. In addition, the wood samples have uniform and predictable pore space, and the orientation of wood cells has influenced the orientation of carbonate veins, making it easier to determine the generations of mineralization and diagenesis, and to define cross-cutting relationships.

3. RESULTS

3.1 Forms of Pyrite

Three forms of pyrite occur in cordaitean peat from the Williamson No. 3 mine in Iowa: 1) small euhedral pyrite found in wood and in the peat matrix (Fig. 4a); 2) framboidal pyrite found in the peat matrix (Fig. 4b); 3) massive anhedral accumulations of pyrite replacing carbonate fabrics, occasionally associated with cracks in the coal ball (Fig. 4c). Small euhedral pyrite crystals often occur inside cells. In some cases, small euhedral pyrite crystals indicate the presence of open pits (pores in plant cells that enable fluids to move between cells) in tracheids and parenchyma cells (Fig. 4a). This pyrite must have formed in early diagenesis, before calcite filled the cell lumina. The cell lumen (plural, lumina) is the space enclosed by the plant cell wall. In rare cases, framboidal structure is preserved (Fig. 4b); most framboidal pyrite occurs in the peat matrix of pristine leaf peat, rather than within plant cells. In samples of wood peat and in the pristine leaf mat, calcite 1 engulfs small euhedral pyrite crystals and framboidal pyrite. The third form of pyrite, massive anhedral pyrite, occurs along cracks and cuts across cell walls (Fig. 4c). Massive anhedral pyrite may replace all carbonate fabrics in certain Williamson No. 3 mine coal balls.

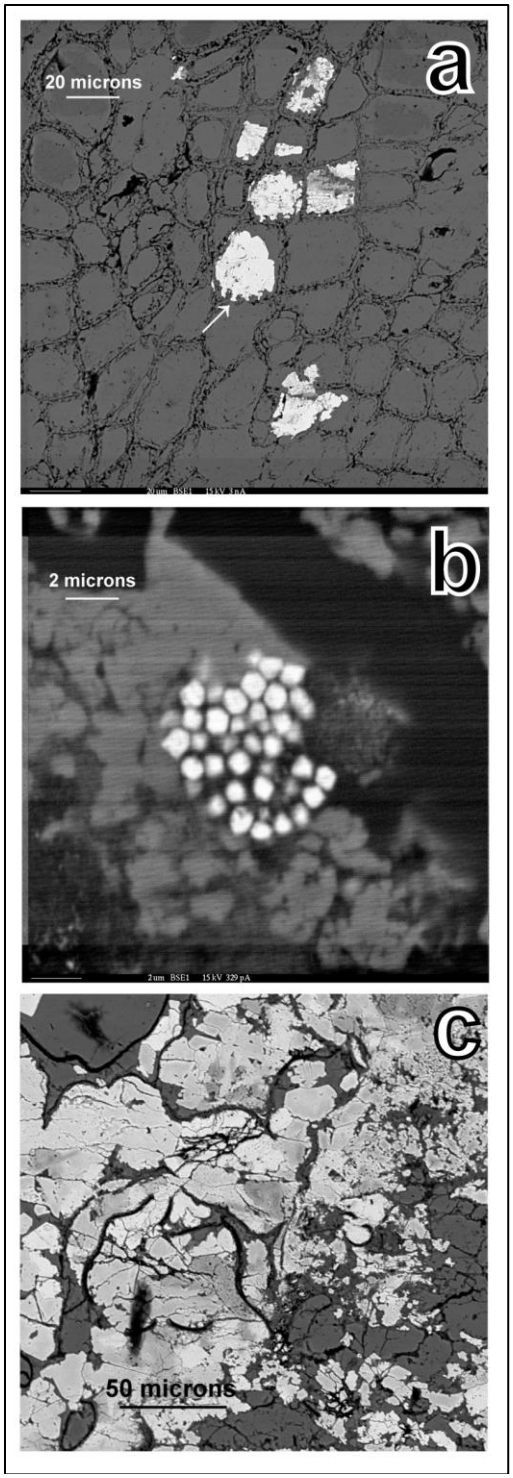

Figure 4. **Pyrite.** a) BSE image of pyrite in the decayed leaf sample preserving pits in cell walls (arrow). b) BSE image of framboidal pyrite in the pristine wood sample. c) BSE image of massive pyritization in a pristine leaf mat.

3.2 Carbonate Fabrics

Six carbonate fabrics occur in *Cordaites*-dominated coal balls from the Williamson No. 3 Mine.

Calcite 1.—This fabric consists of non-ferroan HMC polycrystals with an unusual triangular shape in the basal plane, perpendicular to the c-axis (Fig. 5a-d). These polycrystals have rims of LMC that can be either ferroan or non-ferroan, which make the unusual triangular shape of the polycrystals more pronounced. The HMC of calcite 1 contains between 7.8-16.8 mole% Mg, <0.05-1.06 mole% Fe, and 500-1550 ppm Sr. The LMC rims have Mg contents ranging from 0.2-5.0 mole%, Fe contents ranging from <0.05-2.56 mole%, and <200-990 ppm Sr (Tables 1-3).

The HMC cores of calcite 1 polycrystals consist of micron-sized crystals (Fig 5e). When examined at high magnification using the BSE detector on the SEM, individual crystals within the HMC cores have different grey values, suggesting that they contain varying amounts of magnesium (Fig 5e). The HMC cores of calcite 1 polycrystals also contain micro-dolomite rhombs. The LMC rims of calcite 1 polycrystals have larger crystals than the cores, 10-20μm, and prominent vugs (Fig. 5d-e).

Calcite 1 occurs in all *Cordaites*-dominated coal balls, and is the major permineralizing fabric in cordaitean wood and leaf peats. It fills most tracheids and natural cavities in plant organs (e.g. pith cavities, seed cavities and sporangia). It also fills cavities formed by decomposition (e.g. the open areas between the vascular bundles in leaves created by the decomposition of the leaf mesophyll cells) and interparticle pore

space between leaves and roots. This fabric contains approximately 15% vuggy porosity in cores and rims (Fig. 5d-e).

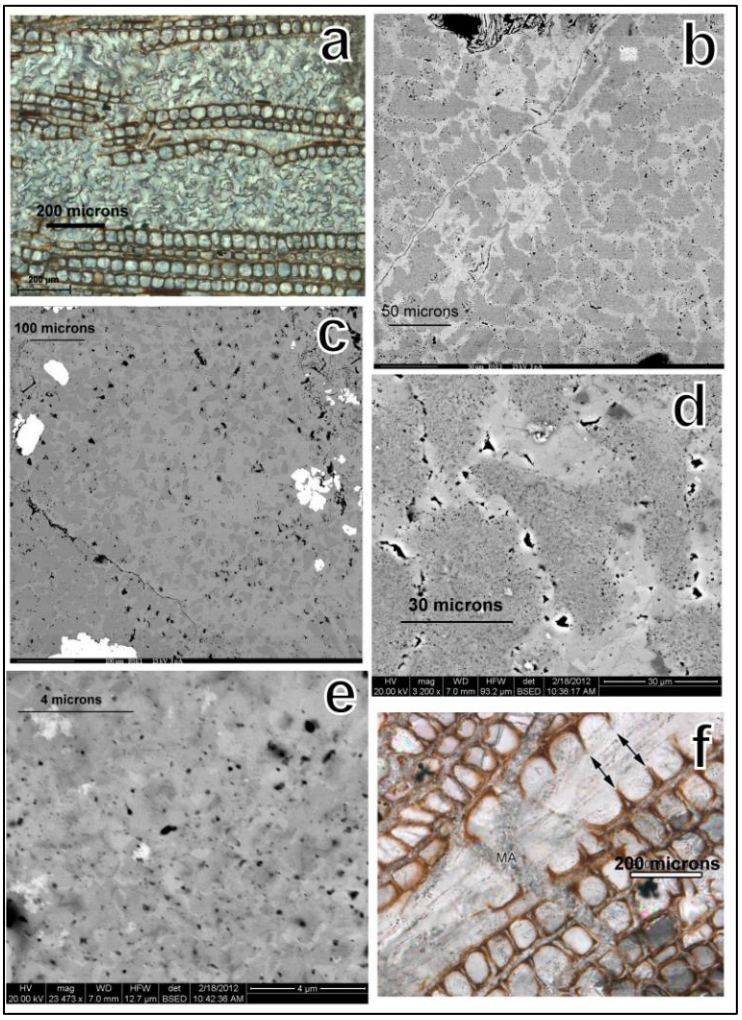

Figure 5. **Calcite 1.** a) Micrograph of triangular shape viewed down the c-axis of calcite 1 polycrystals in the decayed wood sample. b) BSE image of triangular calcite 1 polycrystals with a higher amount of retained HMC in the matrix rich sample. c) BSE image of calcite 1 polycrystals in the decayed leaf sample where much of the HMC was replaced by LMC rims. d) BSE image of grain size differences in HMC cores and LMC rims. e) BSE image of micron-sized grains in the HMC cores of calcite 1 polycrystals. f) Micrograph of decayed wood showing a narrow vein of calcite 1 that has ripped apart tracheid walls in formation; arrows designate broken tracheid walls.

Microcrystalline Calcite A—This fabric consists of microcrystalline LMC, which is generally ferroan but which may be non-ferroan, with rare islands of calcite that are higher in magnesium. The LMC regions have Mg content ranging from 0.25-3.68 mole%, Fe content ranging from 0.1-2.06 mole%, and Sr content ranging from <200-1100 ppm. The HMC regions have Mg content ranging from 4.13-8.1 mole%, Fe content ranging from <0.05-1.1 mole%, and Sr content ranging from <200-770 ppm (Tables 1-3).

Microcrystalline calcite A fills veins in the wood and leaf peats, and small spaces between leaves and other plant organs. In veins, individual crystals range from 10-20μm in size; in cell walls, crystals are often smaller, 5-10μm across. In the decayed wood sample, this fabric fills the narrow pore spaces between tracheid walls. Microcrystalline calcite A appears to permineralize most cell walls. Micron-sized crystals of microcrystalline calcite A have formed within the cell walls of tracheids, fragmenting the walls (Fig. 6a). This fabric also permineralizes parenchyma cells in roots, and the vascular bundle supports of *Cordaites* leaves (Fig. 6b). Dolomite rims are often present around leaf and wood cells that have been permineralized by microcrystalline calcite A (Fig. 6b-c). Finally, microcrystalline calcite A forms spheroids and ovoids in parenchyma cells of wood (ray cells) and leaves that are filled with organic carbon (Fig. 6d).

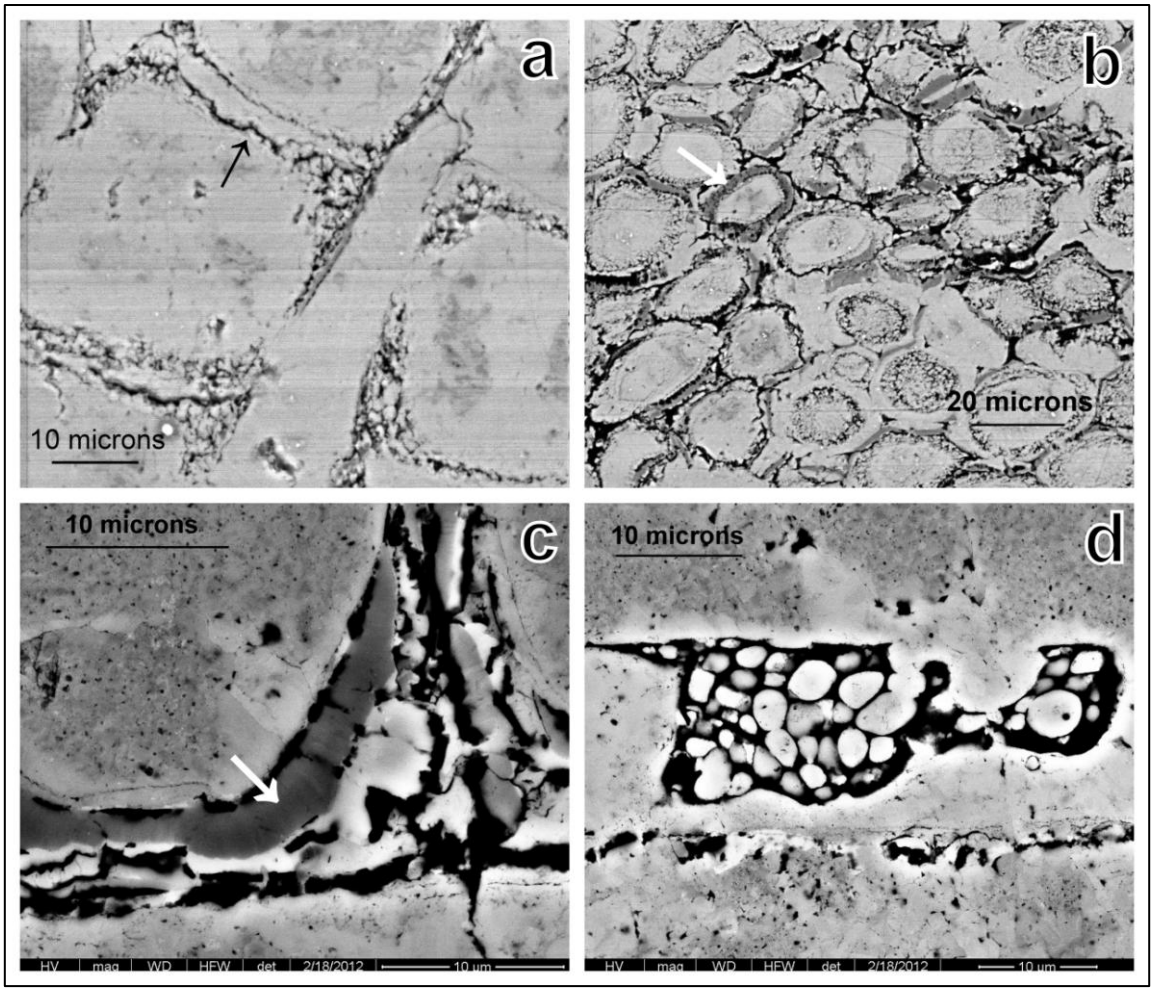

Figure 6. **Microcrystalline Calcite A.** a) BSE image of microcrystalline calcite A in cell walls (arrow) and between pulled apart root tracheids in the pristine leaf sample. b) BSE image of microcrystalline calcite A in vascular bundle supports of leaves in the pristine leaf sample. Dark rims are dolomite (arrow). c) BSE image of wood tracheid with a dolomite rim (arrow) in the decayed wood sample. d) BSE image of spheroids and ovoids in a wood ray cell surrounded by dense organic carbon in the decayed wood sample.

Radial Fibrous Calcite.—Radial fibrous calcite consists of ferroan LMC with islands of non-ferroan HMC (Fig 7a-b). The ferroan LMC of radial fibrous calcite ranges from

0.55-4.92 mole% Mg, 0.55-2.4 mole% Fe, and <200-710 ppm Sr; HMC ranges from 8.54-15.58 mole% Mg, <0.05-0.4 mole% Fe, and 470-940 ppm Sr (Tables 1-3).

BSE images of radial fibrous calcite veins in decayed wood reveal a microcrystalline fabric similar to the HMC cores of calcite 1 polycrystals, suggesting that radial fibrous calcite is a neomorph of calcite 1 (Fig. 5e; Fig. 7b). The HMC grains are micron scale in size and the LMC rims range from 5-10 μm across.

Radial fibrous calcite occurs only in the pristine and decayed wood samples. This fabric always forms linear crystals at the edge of veins that grow inward from both sides. Wide veins have a rim of radial fibrous calcite surrounding calcite 1. Narrow veins may be entirely filled with radial fibrous calcite (Fig. 7c). In some veins, there is typically a seam in the middle where the two edges of radiating crystals meet. In the decayed wood, the centers of veins filled with radial fibrous calcite sometimes contain microcrystalline calcite B or clear anhedral calcite (Fig. 8a).

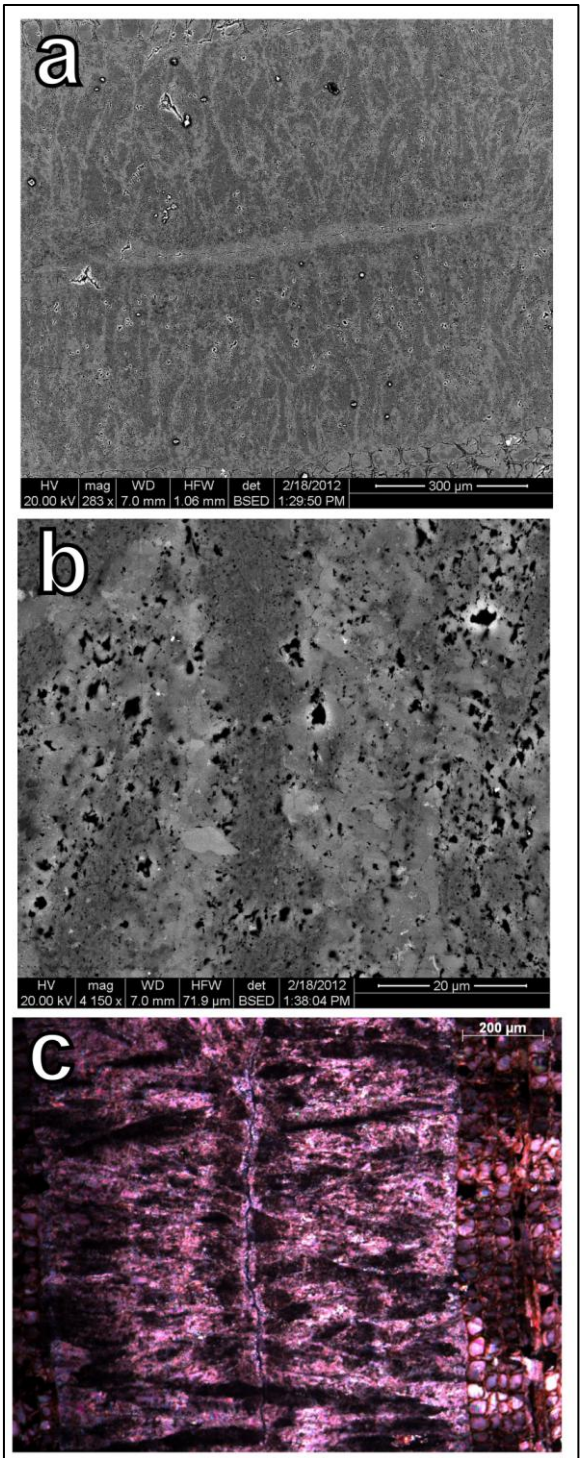

Figure 7. **Radial Fibrous Calcite.** a) BSE image of a radial fibrous vein in the decayed wood sample. b) BSE image of radial fibrous HMC cores and LMC rims. c) Micrograph with crossed nicols of a radial fibrous vein in the decayed wood sample.

Microcrystalline Calcite B.—Microcrystalline calcite B consists of non-ferroan HMC and ferroan LMC with a high volume of finely disseminated decayed organic matter and small euhedral pyrite crystals (Fig. 8b). The LMC phase contains between 1.66-2.21 mole% Mg, 1.46-1.71 mole% Fe, and <200-400 ppm Sr. The HMC phase contains between 7.64-14.66 mole% Mg, <0.05-0.4 mole% Fe, and 530-830 ppm Sr (Tables 1-3). Individual crystals range from 10-20 μm in size.

Microcrystalline calcite B fills narrow veins in the wood, which sometimes expand when crossing veins of calcite 1 (Fig. 8b). Frequently, veins of microcrystalline calcite B have rims of radial fibrous calcite. In veins of microcrystalline calcite B without radial fibrous calcite rims, the microcrystalline calcite B at the edge of the veins has more organic particles making it darker in color (Fig. 8a).

Permineralizing Anhedral Calcite.—Permineralizing anhedral calcite consists of ferroan LMC with occasional small islands of non-ferroan HMC (Fig. 9a). The LMC regions contain 0.3-3.71 mole% Mg, 0.6-3.23 mole% Fe, and <200-700 ppm Sr. The HMC regions contain 12.05-14.28 mole% Mg, <0.05-0.5 mole% Fe, and 650-1410 ppm Sr (Tables 1-3).

The grain size is of permineralizing anhedral calcite ranges from small (<10 μm in diameter) to large (~ 100 μm in diameter), and grains often have curved boundaries (Fig. 9b-c). This fabric is the most common fabric in matrix peat, but also occurs in matrix-rich areas of leaf and wood peat, which consist of small organic particles and have small pore spaces.

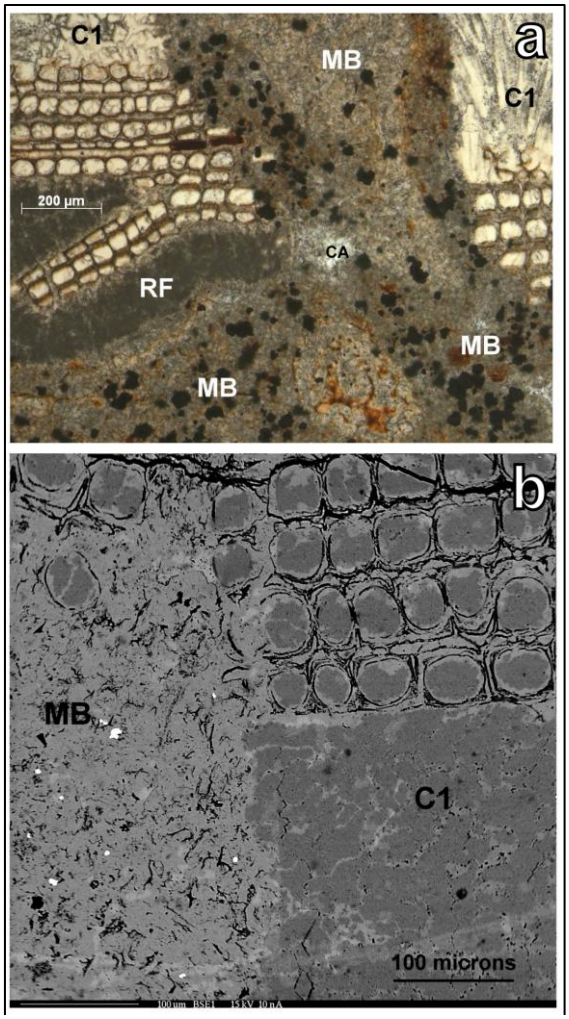

Figure 8. **Microcrystalline Calcite B.** a) Micrograph of a vein of microcrystalline calcite B (MB) lined with radial fibrous calcite (RF) crossing a vein of calcite 1 (C1) in the decayed wood sample. A small patch of clear anhedral calcite (CA) is present in the microcrystalline calcite B vein. b) BSE image of a microcrystalline calcite B (MB) vein cutting a vein of calcite 1 (C1) in the decayed wood sample.

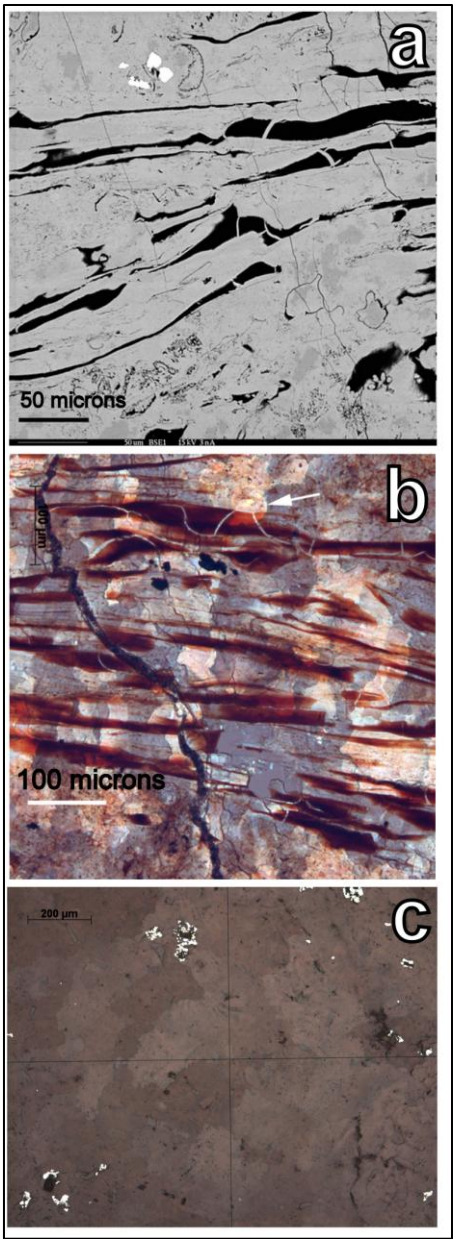

Figure 9. **Permineralizing Anhedral Calcite.** a) BSE image of permineralizing anhedral calcite in the matrix rich sample. b) Micrograph of permineralizing anhedral calcite in the matrix rich sample under crossed nicols. Arrow marks a curved grain boundary. c) Micrograph of permineralizing anhedral calcite in reflected light from the matrix rich sample.

Clear Anhedral Calcite.—Clear anhedral calcite is non-ferroan LMC containing between 1.55-3.25 mole% Mg, <0.05-0.05 mole% Fe, and <200-340 ppm Sr (Tables 1-3). This fabric forms 50-200 μm anhedral calcite crystals without color or organics (Fig. 10a) and occurs at the intersection of veins in decayed wood peat (Fig. 8a) and in veins that cut across fabrics in other peat types (e.g. *Psaronius* root peat).

3.3 Paragenetic Sequence

Fig. 11 shows the paragenetic sequence of coal balls from the Williamson No. 3 Mine. Cross-cutting relationships in the two wood samples and the pristine leaf mat enabled us to place framboidal pyrite, small euhedral pyrite crystals, calcite 1, microcrystalline calcite A, radial fibrous calcite, microcrystalline calcite B, clear anhedral calcite, and massive pyrite in the paragenetic sequence. Permineralizing anhedral calcite, which contains islands of HMC, clearly occurs after calcite 1 in the paragenetic sequence, but does not cut across other calcite fabrics. The curving grain boundaries and wide range of grain sizes in permineralizing anhedral calcite suggest that this fabric results from burial diagenesis (Tucker and Wright, 1990). The presence of islands of HMC suggests that it results from burial diagenesis of calcite 1. Accordingly, we place permineralizing anhedral calcite relatively late in the paragenetic sequence. Massive anhedral pyrite can replace all carbonate fabrics in certain Williamson No. 3 coal balls, and occurs after the formation of permineralizing anhedral calcite. We discuss the placement of clear anhedral calcite in the paragenetic sequence below.

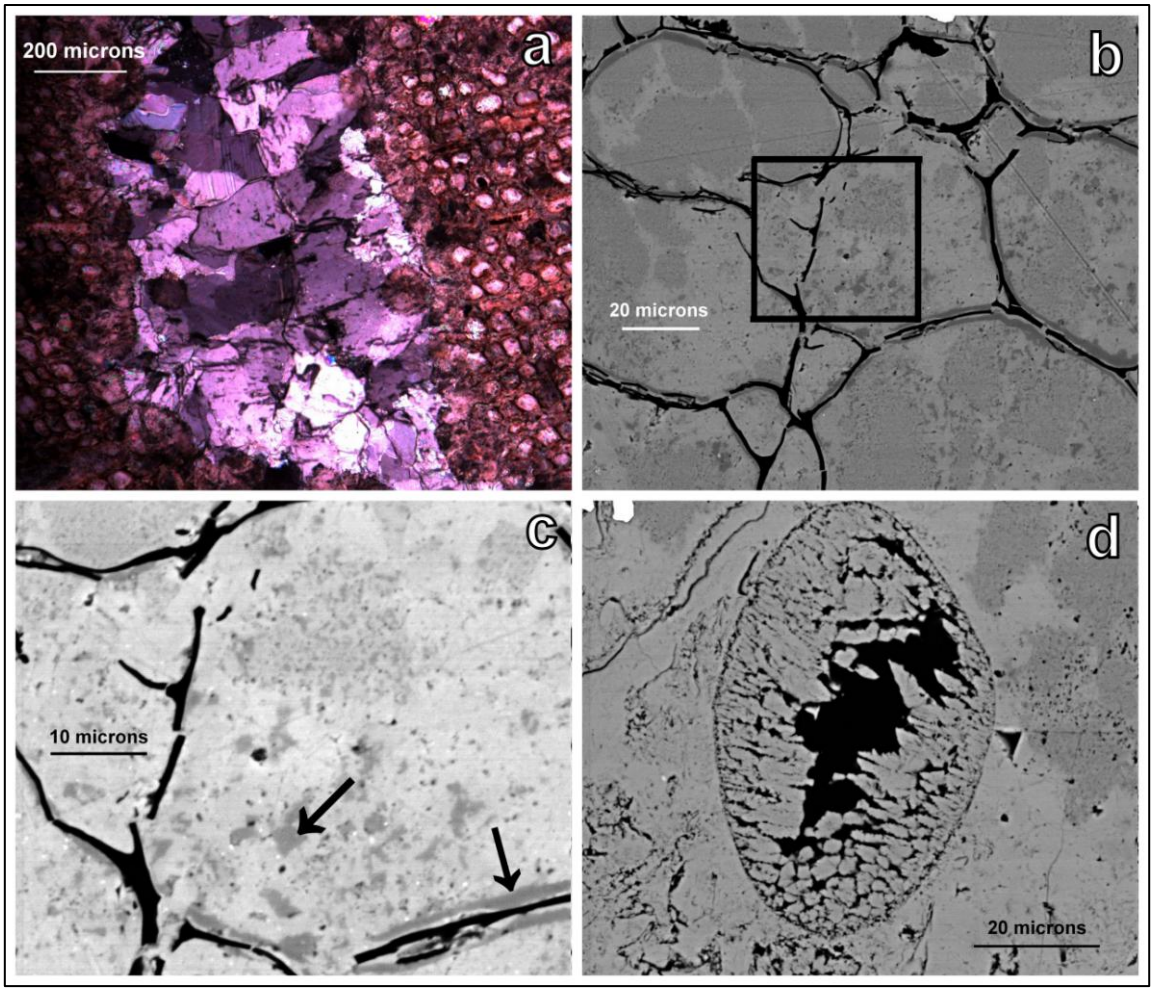

Figure 10. **Clear Anhedral Calcite, Fusain, Geode-like Structure.** a) Micrograph with crossed nicols of clear anhedral calcite in the decayed wood sample. b) BSE image of fusainized tracheids from the pristine leaf sample. Tracheids are filled with calcite 1 and have thin dolomite rims. Box marks region c. c) Closer BSE image of the same area of fusainized tracheids from the pristine leaf. Dolomite rims (arrow) are pronounced and small dolomite rhombs (arrow) occur in the interior of the tracheids. d) BSE image of a geode-like structure filling a leaf fiber cell.

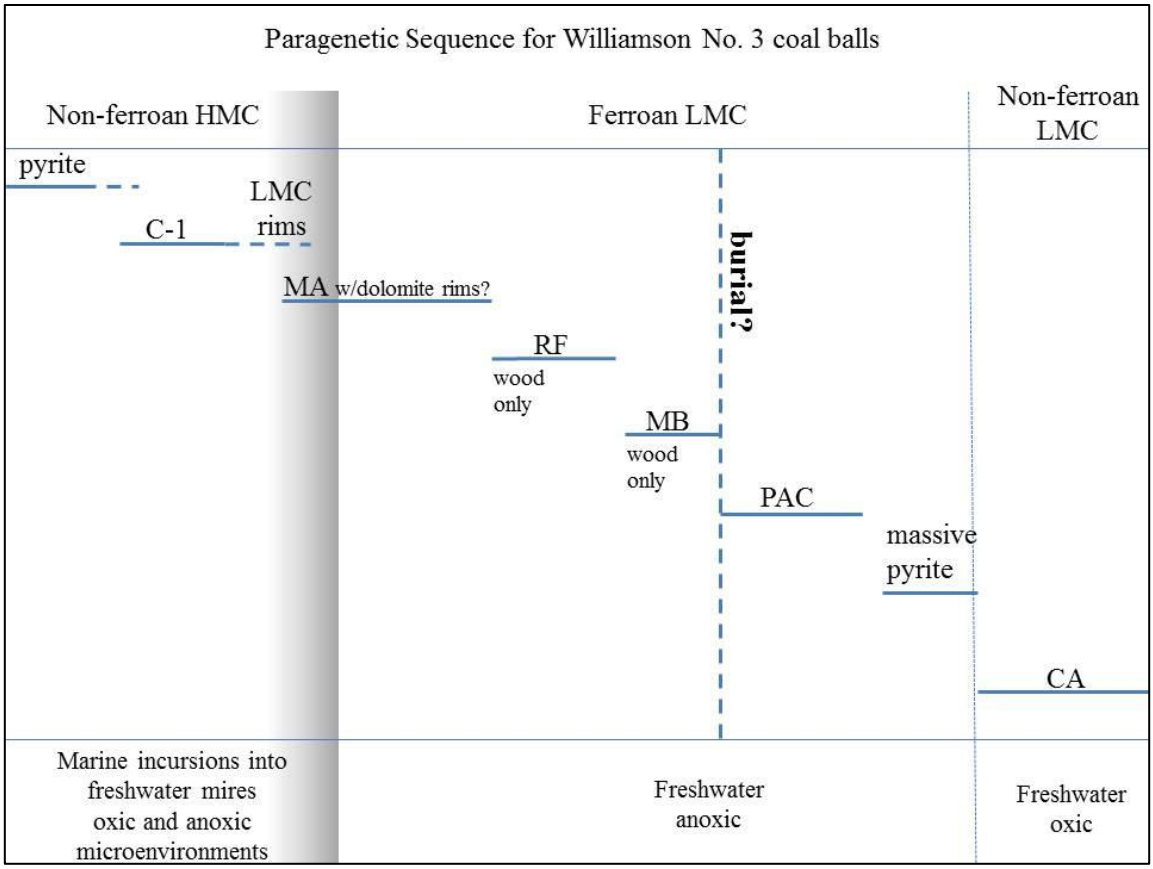

Figure 11. **Paragenetic sequence for the Williamson No. 3 Coal Balls.** C1= calcite 1; MA= microcrystalline calcite A; Dolo= dolomite; RF= radial fibrous calcite; MB= microcrystalline calcite B; PAC= permineralizing anhedral calcite; CA= clear anhedral calcite.

4. DISCUSSION

The trace minerals and the magnesium, strontium and iron content of carbonate fabrics in coal balls from the Williamson No. 3 Mine indicate their environment of formation. Small euhedral pyrite crystals in plant cells and framboidal pyrite in peat and coal indicate the presence of brackish water during, or soon after peat accumulation (Spackman and Cohen, 1977; Horne et al., 1978; Howarth, 1979; Altschuler et al., 1983). HMC with high strontium levels forms from marine water; LMC with low strontium levels forms in freshwater (Tucker and Wright, 1990). Ferroan calcite (Fe > 0.5 mol %) precipitates from anoxic fluids; calcite that precipitates in water containing dissolved oxygen has low Fe levels (Tucker and Wright, 1990). In marine carbonates, ferroan LMC often forms during burial diagenesis (Tucker and Wright, 1990). However in anoxic peat substrates, ferroan LMC could form during early diagenesis from anoxic pore waters. In peat deposits, the catotelm is the lower, anoxic zone of the peat that lies below the permanent water table (Clymo, 1983). Early diagenetic calcite that formed in the catotelm would be expected to be ferroan LMC. The acrotelm is the upper, oxygenated layer of the peat, which generally lies above the permanent water table. Due to seasonal fluctuations in the height of the mire water table, which occur even in tropical mires, the acrotelm-catotelm transition experiences both anoxic and oxic microenvironments (Bragg, 1997; Takahashi and Yonetani, 1997). Thus, ferroan and non-ferroan LMC could have formed in the acrotelm during early diagenesis.

Small euhedral pyrite crystals in Williamson No. 3 coal balls occur within cells and extend into, and in some cases through, open pits, indicating that this pyrite

precipitated before carbonate filled the cells. As previously discussed, framboidal pyrite generally forms during early diagenesis (Howarth, 1979; Kenrick and Edwards, 1988; Grimes et al., 2002). In these coal balls, small euhedral pyrite crystals and framboidal pyrite occur in all carbonate fabrics except radial fibrous calcite, suggesting that both formed before carbonate permineralization. Small euhedral pyrite crystals and framboidal pyrite in peat indicate the presence of brackish or marine water in the mire (Horne et al., 1978; Altschuler et al., 1983).

The earliest carbonate fabric in Williamson No. 3 coal balls consists of calcite 1 polycrystals with HMC cores and LMC rims that are usually ferroan, but which may be non-ferroan. Calcite 1 is the earliest carbonate fabric in the paragenetic sequence for two reasons: it is cross-cut by all other carbonate fabrics except permineralizing anhedral calcite; and all other carbonate fabrics except clear anhedral calcite contain islands of HMC, suggesting that they formed in part due to diagenetic alteration of calcite 1 (Raymond et al., 2012: Fig. 6a; 7a-b; 8b; 9a). Magnesium and strontium concentrations in the HMC cores of calcite 1 polycrystals indicate precipitation in marine water. The LMC rims indicate early diagenesis in meteoric water that was usually anoxic, resulting in ferroan LMC rims, but which occasionally contained oxygen, resulting in non-ferroan LMC rims. Non-ferroan LMC rims occur only in the pristine leaf mat and decayed wood samples, suggesting that these samples lay at the boundary between the acrotelm and catotelm during permineralization. Calcite 1 in all other samples appears to have formed in the catotelm.

High-Mg calcite 1 fills large voids in all peat types, but occurs most commonly in wood and pristine leaf peat. In all peat types, calcite 1 fills the lumina of tracheids (the water-conducting cells of wood), which have porous walls. In matrix peat, calcite 1 occurs in roots and burrows that may have acted as conduits, introducing marine water into decomposed peat of the catotelm, which had smaller particles and low porosity. Thus the abundance of calcite 1 may be a permeability signal, indicating connected pore spaces within peat at the time of permineralization.

The distribution of calcite 1 and microcrystalline calcite A within cell lumina supports the hypothesis that calcite 1 formed in connected pore spaces. In wood, both the parenchymatous ray cells and tracheids have pits (Esau, 1977); and in cordaitean wood samples calcite 1 fills nearly all tracheids and most parenchymatous ray cells. However, ray cells that are filled with organic carbon, decreasing their permeability, contain microcrystalline calcite A, a ferroan LMC, rather than calcite 1. Similarly, in pristine *Cordaites* leaves, calcite 1 fills the space between vascular bundles that was originally occupied by thin-walled mesophyll cells, whereas microcrystalline calcite A fills the thick-walled fibers of the vascular bundle supports, which do not have porous walls, and epidermal cells occluded with organic carbon. Thin-walled parenchyma cells (e.g. root cortex cells and leaf mesophyll) may be filled with calcite 1 or with microcrystalline calcite A.

The growth of calcite 1 polycrystals broke cells walls in the decayed wood specimen (Fig 6f). Calcite 1 also formed displacive arrays of radiating polycrystals at the lower edge of the pristine leaf mat, which are surrounded by zones of poorly

preserved, incompletely permineralized peat. The largest radiating arrays of calcite 1 in our samples grew down from the well-preserved leaf mat into a region of matrix rich peat (i.e. peat composed of unidentifiable plant fragments, many of which are less than 100 μm in their largest dimension: Cohen and Spackman, 1977).

Calcite 1 polycrystals have an unusual growth habit that has only been observed in coal balls from the Williamson No. 3 Mine, seen best in planar section perpendicular to the *c*-axis, (Raymond et al., 2012: Fig 5a-c). However, calcite 1 polycrystals from coal balls are similar in shape to HMC polycrystals precipitated experimentally from fluids containing malic acid by Meldrum and Hyde (2001), and to naturally-occurring HMC polycrystals in subsurface sediments between the saltmarsh and coastal dunes in the area of Grand Isle, LA, found by Kocurko (1980; 1982) and pictured by Given and Wilkinson (1985). In both cases, the distinctive shape of these modern HMC polycrystals may result from the presence of organic acids during calcite precipitation. Calcite 1 polycrystals from coal balls do not retain the internal structure of the polycrystals precipitated by Meldrum and Hyde (2001) or found by Kocurko (1980, 1982: Fig 5e). However, calcite 1 polycrystals may be pseudomorphs of similar HMC polycrystals precipitated from fluids containing organic acids.

The presence of significant amounts of abiotic HMC in coal balls from the Williamson No. 3 Mine is surprising. However, Zodrow et al. (2002) described HMC in coal balls from the Donetz Basin of Russia. BSE images of calcite 1 reveal vuggy HMC cores with tiny crystals and possible microdolomite surrounded by LMC rims with larger crystals (Fig. 5d-e). These LMC rims may have shielded HMC cores of calcite 1 from

diagenetic alteration. In coal balls with large amounts of permineralizing anhedral calcite, a ferroan LMC, the HMC cores of calcite 1 polycrystals are often very small (Fig. 5e), and the eventual fate of calcite 1 polycrystals may be to become radiating arrays of bladed calcite as observed by Schopf (1975), Brownlee (1973), and Rao (1979) in coal balls from the Illinois Basin. These early studies did not report the magnesium content of the bladed calcite crystals.

The next fabric in the paragenetic sequence, microcrystalline calcite A, has a freshwater magnesium and strontium signature. Microcrystalline A is generally ferroan, but may be non-ferroan in the pristine leaf mat sample. As previously discussed, this fabric occurs in the lumina of cells occluded with organic carbon and cells with nonporous walls. It also appears to be the original permineralizing fabric of cell walls including parenchyma cells, fiber cells in the vascular bundle supports of *Cordaites* leaves, and tracheids (Fig. 6). Some microcrystalline calcite A results from diagenetic alteration of calcite 1: veins of microcrystalline calcite A in the pristine leaf mat and decayed wood have islands of HMC, indicating that the original permineralizing fabric was calcite 1. In some regions of the decayed wood sample, the microcrystalline calcite A found between tracheids in the position of the missing middle lamina contains islands of HMC and may result from the diagenetic alteration of calcite 1. However, in other parts of this specimen microcrystalline calcite A does not have regions of HMC and may have been the original permineralizing fabric (Raymond et al., 2012).

Raymond et al. (2012) suggested that the fluids responsible for the precipitation of microcrystalline calcite A also formed the LMC rims of calcite 1 polycrystals. The

LMC rims of calcite 1 polycrystals in decayed wood and pristine leaf peat and microcrystalline calcite A in the pristine leaf mat are the only LMC fabrics that have variable iron content, suggesting that these samples lay at the boundary between the acrotelm and catotelm when they experienced meteoric diagenesis. Variable iron contents in the LMC rims of calcite 1 and in microcrystalline calcite A suggest that both formed early in diagenesis. Our paragenetic sequence implies that the cell lumina of tracheids and ray cells in wood and root cortex cells filled with calcite 1 before permineralization of the cell walls.

The fiber cells of *Cordaites* leaves permineralized by microcrystalline calcite A often have thin dolomite rims (Fig. 6b). Dolomite occasionally rims cavities between fiber cells, suggesting that these were open pores at the time of dolomite formation. However, the rims are not continuous around all fiber cells, suggesting that rims formed after initial compaction and deformation of the fiber cells. Raymond et al. (2012) reported that dolomite rims occurred only associated with the fiber cells of *Cordaites principalis* leaves; however, new research suggests that narrow dolomite rims also occur in decayed cordaitean wood and in tracheids from the pristine leaf mat (Fig. 6b-c). Zodrow et al. (2002) observed dolomite rims in coal balls from the Donetz Basin. Less frequently, dolomite rhombs are present in the LMC rims of calcite 1 (Fig. 10c). Though coal balls from the Kalo formation have retained a significant amount of their original HMC, most remaining HMC is rimmed by LMC, which may have acted as a shield to further diagenetic alteration.

The next two fabrics in the paragenetic sequence, radial fibrous calcite and microcrystalline calcite B, are ferroan LMC with islands of HMC (Fig 7a; 8b). They are constrained in the paragenetic sequence by cross-cutting relationships defined in the decayed wood sample. Both are considered neomorphs of calcite 1 that formed in fresh pore waters because they contain islands of HMC. Radial fibrous and microcrystalline calcite B occur only in large cracks in wood, and microcrystalline calcite B is specific to the decayed wood sample. Both radial fibrous calcite and microcrystalline calcite B fill radial and tangential veins in decayed *Cordaites* wood. Veins filled with microcrystalline calcite B are narrow in wood and may expand when cutting across calcite 1veins, suggesting that the presence of tracheid walls and microcrystalline calcite A constrained the formation of microcrystalline calcite B veins (Fig 3b).

Permineralizing anhedral calcite forms in matrix rich peat and in decayed leaf mats, which have small pores and probably low permeability. It also occurs in matrix rich regions of the pristine leaf mat and wood peat. It is primarily ferroan LMC, but may contain small islands of HMC, suggesting that some permineralizing anhedral calcite is a neomorph of calcite 1. This fabric has curving grain boundaries and a wide range in grain sizes consistent with burial diagenesis (Tucker and Wright, 1990; Fig 9b). The placement of permineralizing anhedral calcite in the paragenetic sequence is not constrained by cross-cutting relationships with other fabrics. It is placed late in the paragenetic sequence because it is the only carbonate fabric in Williamson No. 3 coal balls that appears to result from burial diagenesis (Tucker and Wright, 1990).

Some coal balls from the Williamson No. 3 Mine experienced secondary pyritization by massive anhedral pyrite, which affects all carbonate fabrics in these coal balls. This pyrite forms preferentially along fractures and on the edges of coal balls as a result of a change in pore water geochemisty after the formation of permineralizing anhedral calcite (Fig. 4c).

The final fabric in the paragenetic sequence is clear anhedral calcite, which is LMC with the lowest levels of strontium and by far the lowest levels of iron compared to the other carbonate fabrics. It is completely free of organic matter and probably formed after coalification of the Williamson No. 3 coal deposit, from fresh, meteoric pore water in the presence of oxygen.

4.1 Cellular Controls on Carbonate Permineralization

BSE images provide new insight into the process of permineralization (Scott and Collinson, 2003; Boyce et al., 2010). The features of tracheids are preserved with the most detail by early diagenetic pyrite, which can fill cells, forming molds of the pits in tracheid walls (Fig. 4a). In peat permineralized by calcium carbonate, cell walls are commonly preserved by microcrystalline calcite A. Micron-sized calcite crystals regularly break up tracheid walls during permineralization, frequently destroying detailed features such as pits (Fig. 6a). Fossil charcoal (fusain) is an exception. Tracheid walls of fusainized wood are surrounded by microcrystalline calcite A, but appear solid and are not interrupted by micron-sized crystals (Fig. 10b-c). Tracheid walls of fusainized wood often have thin dolomite rims (Fig. 10c). In BSE images, the distinction

between burned and decayed tracheids within coal balls is immediately apparent (Figs. 6a; 10b-c).

In contrast to tracheid walls, the cell walls of collenchyma fibers in the vascular bundle supports of *Cordaites* leaves are preserved as solid rims of microcrystalline calcite A with micron-sized calcite crystals and organic carbon filling the cell lumina. These two different styles of cell wall preservation suggest different original cell wall configurations and compositions: porous and lignitic for tracheids, non-porous and cellulosic for collenchyma fibers in *Cordaites* leaves (Esau, 1977).

Raymond et al. (2012) noted the correlation between large pores, permeability and calcite 1 (HMC) in Williamson No. 3 coal balls. However, because most subsequent carbonate fabrics in coal balls incorporate some calcite 1, as evidenced by the persistence of islands of HMC, they felt that HMC may have occurred widely but is preserved today only in wood and large pore spaces. The correlation between cell wall porosity and carbonate fabrics suggests that the presence of calcite 1 filling large pore spaces in permeable peat and conduits in less permeable matrix rich peat, such as wood and burrows, reflects its original distribution and is not a diagenetic signal. We also recognize that even in surficial leaf mats, which must have been among the most permeable Pennsylvanian peats, cell walls and certain cells (lumina, collenchyma, fiber and parenchyma cells filled with organic matter) are permineralized by microcrystalline calcite A.

Parenchyma cells are typically well preserved and look, in general, like thin-walled fossil charcoal. Cells filled with organic carbon display several different forms of

calcite, which may be linked to the types of organic acids present in each cell (Meldrum and Hyde, 2001). Some parenchyma cells in wood and leaves are filled with small spheres and chains of spheres composed of microcrystalline calcite A in a dense organic matrix (Fig. 6d). These spheres may preserve the shape of fungal hyphae that attacked cells in life or after death. Possibly, they occur widely in coal balls, but can only be discerned in cells filled with organic matter; or, the organic carbon filling these cells may have been a response to fungal infection. Cohen and Spackman (1980) documented the infilling of parenchyma cells and water conducting cells of peat constituents after death during coalification. Other filled parenchyma cells exhibit jagged geode-like structures with dense organic matter in the center (Fig.10d). As previously described, the lumina of collenchyma cells are filled with micron-sized calcite crystals and organic matter. The different types of carbonate crystals filling individual cells are complex and not fully understood.

Although permineralizing anhedral calcite apparently results from burial diagenesis, its distribution correlates with the occurrence of matrix rich peat. Islands of HMC within permineralizing anhedral calcite suggest that some is a neomorph of calcite 1. However, in the degraded leaf mat and matrix rich samples, most permineralizing anhedral calcite consists of LMC with finely disseminated organic matter and plant fibers. Permineralizing anhedral calcite, which is ferroan LMC, may be a neomorph of microcrystalline calcite A. If so, microcrystalline calcite A may have been the predominant carbonate fabric in low porosity, low permeability peat. However based on strontium and iron content, the HMC and LMC regions of permineralizing anhedral

calcite most closely resemble the geochemical composition of calcite 1 HMC cores and LMC rims (Tables 2-3; Fig 12). Resolution of the source of permineralizing anhedral calcite requires more research.

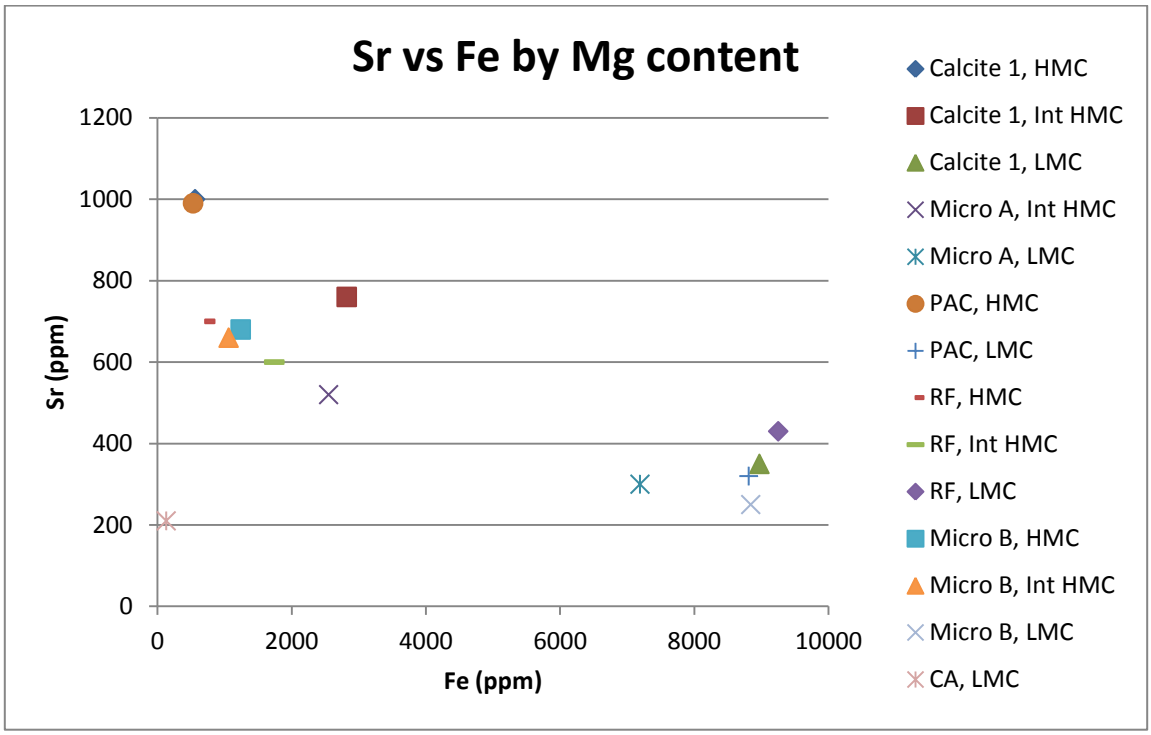

Figure 12. **Strontium vs. Iron plot.** Fabric's separated into LMC, Int HMC and HMC (for values, see Tables 1-3).

4.2 Implications for Coal Ball Formation

A number of mechanisms for coal ball formation have been proposed (Scott et al., 1996). Raymond et al. (2012) outlined three general models of coal ball formation: salt-water incursions into freshwater swamps (Stopes and Watson, 1909; Rao, 1979); introduction of marine pore water into buried freshwater peat (Spicer, 1989); erosional

unroofing of buried peat (DeMaris, 1983). The paragenetic sequence of Williamson No. 3 coal balls suggests that these coal balls formed due to the introduction of marine water into a freshwater swamp. Although the Williamson No. 3 peat probably accumulated in a freshwater mire (Raymond et al., 2010), small euhedral pyrite crystals and framboidal pyrite indicate the occasional presence of marine water in the Williamson No. 3 mire. Sporadic marine incursions acted as a catalyst for the precipitation of HMC (calcite 1) in this predominately fresh water system. Coal-ball carbonates then experienced early meteoric diagenesis, forming the LMC rims of calcite 1, microcrystalline calcite A, radial fibrous calcite and microcrystalline calcite B. Permineralizing anhedral calcite formed in response to burial diagenesis in fresh pore waters, which suggests that the pore waters of the Williamson No. 3 coal remained fresh even after burial. Rao (1979) proposed a similar origin for coal balls from the Illinois Basin. In the Williamson No. 3 deposit, late stage secondary pyritization by anhedral pyrite provides evidence for the introduction of anoxic, iron-rich formational waters during late diagenesis.

The Moscovian sediments of the mid-continent record repeated 4^{th} and 5^{th} order transgressive-regressive cycles (known as cyclothems), probably driven by the advance and retreat of continental ice sheets (Heckel, 1977, 1986). The Kalo Formation preserves two transgressive-regressive cycles that were probably driven by glacial-eustatic sea level fluctuations (Raymond et al., 2010). The carbonate geochemistry of coal balls from the Kalo Formation of Iowa and from the Illinois Basin (Rao, 1979) suggests that they formed in peat deposits that retained fresh pore waters even after

burial by marine sediments. This hypothesis of coal ball formation implies heavy rainfall in Pennsylvanian mires. In areas with significant rainfall, the hydraulic head is high and buried sediments retain fresh pore waters even after marine transgression and burial by marine sediments (Meisler et al., 1988). Salt water enters fresh water formations when the hydraulic head of the fresh water package is low (Meisler et al., 1988). Neuzil et al., (1993) observed fresh pore water in a tropical freshwater peat from Indonesia that had been submerged in marine water due to sea level rise.

This model also requires the deposition of impermeable marine sediments overlying the freshwater sediments that contain the freshwater lens (in the case of the Kalo Formation – peat). Near New Jersey, USA, fresh water wedges in Cretaceous fluvial-deltaic sands, capped by marine confining beds, extend up to 90 km off the coast (Meisler et al., 1988). In the Kalo Formation, marine transgressive shales and carbonates may have acted as confining beds.

In the paragenetic sequence of Williamson No. 3 coal balls, the formation of massive anhedral pyrite marks the introduction of anoxic, iron-rich formational fluids into the system. Clear anhedral calcite, which is also non-ferroan, probably forms from meteoric pore water in the presence of oxygen, after the uplift and exposure of Pennsylvanian strata. In Pennsylvanian coal balls from the Donetz and Illinois Basins, clear anhedral calcite shared the same stable isotopic composition as cleat calcite from the source coals (i.e. calcite formed in cracks in coal seams: Brownlee, 1975; Zodrow et al., 2002).

5. CONCLUSIONS

The distribution of trace minerals and the carbonate petrology and geochemistry of Williamson No. 3 coal balls enable us to determine their environment of formation. Although the Williamson No. 3 coal probably accumulated in a freshwater mire (Raymond et al., 2010), the widespread occurrence of small euhedral calcite crystals and framboidal pyrite in Williamson No. 3 coal balls suggests the presence of salt or brackish water in the mire. The earliest carbonate fabric in our sample set from the Williamson No. 3 Mine consists of HMC polycrystals (calcite 1) with an unusual growth habit, similar to HMC experimentally precipitated from solutions containing malic acids by Meldrum and Hyde (2001) and to modern HMC precipitated adjacent to a saltmarsh along the coast of Louisiana (Kocurko, 1980, 1982; Given and Wilkinson, 1985). The high magnesium and strontium content of this calcite coupled with low iron content indicate precipitation from marine water in the presence of dissolved oxygen. Though the polycrystals have been recrystallized, they retain the general bladed, triangular shape of the Kocurko (1980, 1982) crystals, made even more pronounced by LMC rims, which are generally ferroan but may be non-ferroan in the decayed wood and pristine leaf mat samples. These LMC rims indicate early diagenesis of HMC polycrystals (calcite 1) in meteoric water.

Like the LMC rims of calcite 1, the second carbonate fabric to form, microcrystalline calcite A, is generally ferroan LMC, but may be non-ferroan in the pristine leaf mat. Subsequent generations of calcite in Williamson No. 3 coal balls reflect diagenesis in meteoric water. The curved grain boundaries and wide range of

grain sizes in permineralizing anhedral calcite reflect burial diagenesis in fresh pore water.

Detailed study of carbonate fabrics in relation to plant cell type and the size of peat particles revealed several distinct correlations. Calcite 1 appears to fill pores in porous, permeable peat, while microcrystalline calcite A permineralizes cell walls and fills cells with restricted fluid flow. Permineralizing anhedral calcite is a neomorph of calcite 1 that forms in matrix rich peat. Plant taxonomy and the availability of pore space play an important role in determining the carbonate fabric and diagenetic alteration of coal balls.

Our results have implications for the paleohydrogeology of Pennsylvanian sediments. The diagenetic history of Williamson No. 3 coal balls suggest that this coal maintained a persistent freshwater lens, possibly because the overlying marine shale acted as a confining bed. Meisler et al. (1988) reported persistent freshwater lenses in fluvial-deltaic Cretaceous sediments overlain by marine muds along the coast of New Jersey and suggested that high rainfall during the Cretaceous contributed to the presence and persistence of the freshwater lens.

Our results suggest that many isotopic values previously reported from coal balls have fresh water signatures because the stable isotopic values of the original marine cement, calcite 1, were reset by fresh water that remained in the peat for an extended time after burial. Our results are consistent with Scott et al. (1996), who concluded that the stable isotopes of coal-ball calcite represent mixing between marine and fresh water.

A probable next step in this project is to isolate the HMC regions and the other carbonate fabrics for stable isotopic analyses.

REFERENCES

ALTSCHULER, Z.S., SCHNEFPE, M.M., SILBER, C.C., SIMON, F.O., 1983, Sulfur diagenesis in Everglades peat and origin of pyrite in coal: Science, v. 221(4607), p. 221-227.

ANDERSON, T.F., BROWNLEE, M.E., PHILLIPS, T.L., 1981, A stable isotope study on the origin of permineralized peats zones in the Herrin Coal: Journal of Geology, v. 88, p. 713-722.

BOELTER, D. H., 1969, Physical properties of peat as related to degree of decomposition: Soil Science Society of America Proceedings, v. 33, p. 606-609.

BOYCE, C. K., ALBRECHT, M., ZHOU, D., GILBERT, P.U.P.A., 2010, X-ray photoelectron emission spectromicroscopic analysis of arborescent lycopsid cell wall composition and Carboniferous coal ball preservation: International Journal of Coal Geology**,** v. 83, p. 146-153.

BRAGG, O.M., 1997, Understanding ombrogenous mires of the temperate zone and the tropics: An ecohydrologist's view of tropical peatlands, *in* Rieley, J.O., and Page, S.E., eds., Biodiversity and sustainability of tropical peatlands, Cardigan, U.K., Samara Publishing Ltd., p. 135-146.

BROWNLEE, M.E., 1975, Stable Carbon and Oxygen Isotopes of Carbonate Coal Balls and Associated Carbonates of the Illinois Basin. Unpublished M.S. thesis, University of Illinois at Urbana-Champaign, Champaign, Il, 99 p.

CLYMO, R.S., 1983, Peat, *in* A. P. Gore. Amsterdam, Elsvier Scientific Publishing Company, Ecosystems of the World 4A. Mires: Swamp, bog, fen, and moor: 4A, p. 159-224.

COHEN, A.D., and SPACKMAN, W., 1977, Phytogenic organic sediments and sedimentary environments in the Everglades-mangrove complex: Part II. The origin, description, and classification of the peats of Southern Florida: Palaeontographica Abt. B, v. 162, p. 71-114.

COHEN, A.D., and SPACKMAN, W., 1980, Phytogenic organic sediments and sedimentary environments in the Everglades-mangrove complex of South Florida, Part 3: Alteration of plant material in peat: Palaeontographica Abt. B, v. 172, p. 125-149.

DEMARIS, P.J., 2000, Formation and distribution of coal balls in the Herrin Coal (Pennsylvanian), Franklin County, Illinois Basin, USA: Journal of the Geological Society, London, v. 157, p. 221-228.

DEMARIS, P.J., BAUER, R.A., CAHILL, R.A., DAMBERGER, H.H., 1983, Geologic investigation of roof and floor strata: longwall demonstration, Old Ben Mine No. 24, prediction of coal balls in the Herrin Coal, final technical report part 2: IGS Contract/Grant report, Champaign, Illinois, Illinois Geological Survey, v. 1983-2, p. 77.

ESAU, K., 1977, Anatomy of Seed Plants: John Wiley and Sons, New York, U.S.A., 550 p.

FLUGEL, E., 2010, Microfacies of carbonate rocks: Analysis, Interpretation and Application: Springer, Heidelberg, Germany.

GIVEN, R.K., and WILKINSON, B.H., 1985, Kinetic control of morphology, composition, and mineralogy of abiotic sedimentary carbonates: Journal of Sedimentary Petrology, v. 55, p. 109-119.

GRIMES, S.T., BROCK, F., RICKARD, D., DAVIES, K.L., BRIGGS, D.E.G., EDWARDS, D., PARKER, R.J., 2001, Understanding fossilization: experimental pyritization of plants: Geology, v. 29, p. 123-126.

GRIMES, S.T., DAVIES, K.L., BUTLER, L.B., BROCK, F., EDWARDS, D., RICKARD, D., BRIGGS, D.E., PARKER, R.J., 2002, Fossil plants from the Eocene London Clay: the use of pyrite textures to determine the mechanism of pyritization: Journal of the Geological Society of London, v. 159, p. 493-501.

HECKEL, P.H., 1977, Origin of phosphatic black shale facies in Pennlysvanian cyclothems of mid-continent North America: AAPG Bulletin, v. 61, p. 1045-1068.

HECKEL, P.H., 1986, Sea-level curve for Pennsylvanian eustatic marine transgressive-regressive depositional cycles along midcontinent outcrop belt, North America: Geology, v. 14, p. 330-334.

HORNE, J.C., FERME, J.C., CARRUCCIO, F.T., BAGNEZ, B.P., 1978, Depositional models in coal exploration and mine planning in the Appalachian region: AAPG Bulletin, v. 62(12), p. 2379-2411.

HOWARTH, R.W., 1979, Pyrite: Its rapid formation in a salt marsh and its importance in ecosystem metabolism: Science, v. 203, p. 49-51.

KENRICK, P. and EDWARDS, D., 1988, The anatomy of Lower Devonian Gosslingia breconensis heard based on pyritized axes, with some comments on the permineralization process: Botanical Journal of the Linnean Society, v. 97, p. 95-123.

KOCURKO, J.M., 1980, Early Cementation by High-Magnesium Calcite from Gulf Coast of Louisiana: American Association of Petrolueum Geologists (AAPG), v. 64, p. 734.

KOCURKO, J.M., 1982, Carbonate Cementation of Gulf Coast Barrier-Island Sands and Formation of a Stratigraphic Trap: ABSTRACT: American Association of Petroleum Geologists (AAPG), v. 66, p. 245.

LEVESQUE, M.P. and MATHUR, S.P. 1979, A comparison of various means of measuring the degree of decomposition of virgin peat in the context of their relative biodegradability: Canadian Journal of Soil Science, v. 59, p. 397-400.

MAMAY, S.H. and YOCHELSON, E.L., 1962, Occurrence and significance of marine animal remains in American coal balls: United States Geological Survey Professional Paper, v. 354, p. 193-224.

MEISLER, H., MILLER, J.A., KNOBEL, L.L, WAIT, R.L., 1988, Region 22, Atlantic and eastern Gulf Coastal Plain *in* Back, W., Rosenshein, J.S., and Seaber, P.R., The Geology of North America: The Geological Society of America, Inc., v. O-2, Boulder, Colorado, p. 209-218.

MELDRUM, F. C., and HYDE, S. T., 2001, Morphological influence of magnesium and organic additives on the precipitation of calcite: Journal of Crystal Growth, v. 231, p. 544-558.

NEUZIL, S.G., CECIL, C. B., KANE, J.S., 1993, Inorganic geochemistry of domed peat in Indonesia and its implication for the origin of mineral matter in coal, *in* Cobb, J. C., and Cecil, C. B., eds., Modern and ancient coal-forming environments: Geological Society of America Special Paper 286, Boulder, Colorado, Geological Society of America p. 23-44.

RAO, P.C., 1979, Origin of Coal Balls of the Illinois Basin: 9th International Congress on Carboniferous Stratigraphy and Geology (IX-ICC), p. 393-406.

RAYMOND, A., 2011, Wood decomposition in Paleozoic and modern mires, GSA Abstracts with Program, v. 43(5), p. 500.

RAYMOND, A., GUILLEMETTE, R., JONES, C.P., AHR, W., 2012, Carbonate petrology and geochemistry of Pennsylvanian coal balls from the Kalo Formation of Iowa: International Journal of Coal Geology.

RAYMOND, A., CUTLIP, P.C., SWEET, M., 2001, Rates and processes of terrestrial nutrient cycling in the Paleozoic: the world before beetles, termites, and flies, *in* Allmon, W.D. and Bottjer, D.J., Evolutionary Paleoecology: The Ecological Context of Macroevolutionary Change, Columbia University Press, New York, p. 235-283.

RAYMOND, A., LAMBERT, L., COSTANZA, S.H., SLONE, E.J., CUTLIP, P.C., 2010, Cordaiteans in paleotropical wetlands: An ecological re-evaluation: International Journal of Coal Geology, v. 83, p. 248-256.

RAYNER, A. D. M. and BODDY, L., 1988, Fungal Decomposition of Wood: It's Biology and Ecology: John Wiley and Sons, New York.

SCHOPF, J. M., 1975, Modes of fossil preservation: Review of Palaeobotany and Palynology, v. 20, p. 27-53.

SCOTT, A.C., D. P. MATTEY, D.P., HOWARD, R., 1996, New data on the formation of Carboniferous coal balls: Review of Palaeobotany and Palynology, v. 93, p. 317-331.

SCOTT, A.C. and REX, G., 1985, The formation and significance of Carboniferous coal balls: Philosophical Transactions of the Royal Society of London B: Biological Sciences, v. 311, p. 123-137.

SCOTT, A.C., and COLLINSON, M.E., 2003, Non-destructive approaches to interpret the preservation of plant fossils: implications for calcium-rich permineralizations: Journal of Geological Society, v. 160, p. 857-862.

SPICER, R.A., 1989, The formation and interpretation of plant fossil assemblages: Advances in Botanical Research, v. 16, p. 95-191.

STOPES, M.C. and WATSON, M.S., 1909, On the present distribution and origin of the calcareous concretions in coal seams, known as 'coal balls': Philosophical Transactions of the Royal Society of London B: Biological Sciences, v. 200, p. 167-218.

TAKAHASHI, H., and YONETANI, Y., 1997, Onset and rate of peat and carbon accumulations in four domed ombrogenous peat deposits, Indonesia, *in* Rieley, J. O., and Page, S. E., eds., Biodiversity and sustainability of tropical peatlands, Cardigan, U.K., Samara Publishing Ltd., p. 179-187.

TUCKER, M. E. and WRIGHT, V.P., 1990, Carbonate Sedimentology, Blackwell Scientific Publications, Oxford, England, 482 p.

ZODROW, E.L. and CLEAL, C.J., 1999, Anatomically preserved plants in siderite concretions in the shale split of the Foord Seam: mineralogy, geochemistry, genesis (Upper Carboniferous, Canada): International Journal of Coal Geology, v. 41, p. 371-393.

ZODROW, E.L., LYONS, P.C., MILLAY, M.A., 1996, Geochemistry of autochthonous and hypautochthonous siderite-dolomite coal-balls (Foord Seam, Bolsovian, Upper Carboniferous), Nova Scotia, Canada: International Journal of Coal Geology, v. 29, p. 199-216.

ZODROW, E.L., SNIGEREVSKAYA, N.S., PALMER, C.A., 2002, Paleoenvironments and carbonate processes in plant-tissue preservation of calcite coal balls: Carboniferous and Permian of the World: XIV ICCP proceedings. L. V. Hills, C. M. Henderson and E. W. Bamber. Calgary, Canada, Canadian Society of Petroleum Geologists, v. 19, p. 393-411.

APPENDIX

Tables

Table 1. **Magnesium composition by carbonate fabric.**

	HMC			Int HMC: (4-9.7 mole %, 1-2.5 wt% Mg)			LMC		
Fabric	# of analyses	Ave Mg mole%	Range Mg mole%	# of analyses	Ave Mg mole%	Range Mg mole%	# of analyses	Ave Mg mole%	Range Mg mole%
Calcite 1	196	14.2	11.2-16.8	5	7.11	4.46-9.28	171	1.34	0.2-3.52
Micro A	0	n/a	n/a	5	5.99	4.13-8.1	47	1.49	0.25-3.68
Perm Anhedral	22	13.6	12.1-14.4	0	n/a	n/a	55	1.13	0.3-3.71
Radial Fibrous	19	12.1	9.76-15.6	6	8.4	4.92-9.65	28	1.51	0.55-3.52
Micro B	2	12.9	11.1-14.7	1	7.64	7.64	5	2.05	1.66-2.21
Clear Anhedral	0	n/a	n/a	0	n/a	n/a	5	2.4	1.55-3.25
Totals	238	13.2		17	7.29		311	1.65	

Table 2. **Iron composition by carbonate fabric.** Lower limit of detection is 0.05 mole%.

	HMC			Int HMC: (4-9.7 mole %, 1-2.5 wt% Mg)			LMC		
Fabric	# of analyses	Ave Fe mole%	Range Fe mole%	# of analyses	Ave Fe mole%	Range Fe mole%	# of analyses	Ave Fe mole%	Range Fe mole%
Calcite 1	195	0.1	<0.05-1.06	5	0.48	<0.05-1.35	171	1.61	<0.05-2.56
Micro A	0	n/a	n/a	5	0.43	<0.05-1.1	47	1.32	0.1-2.06
Perm Anhedral	22	0.9	<0.05-0.5	0	n/a	n/a	55	1.59	0.06-3.23
Radial Fibrous	19	0.11	<0.05-0.4	6	0.31	<0.05-1.16	28	1.63	0.55-2.4
Micro B	2	0.23	<0.05-0.4	1	0.2	0.2	5	1.62	1.46-1.71
Clear Anhedral	0	n/a	n/a	0	n/a	n/a	5	0.01	<0.05-.0.05
Totals	238	0.34		17		0.20	311	1.30	

Table 3. **Strontium composition by carbonate fabric.** Lower limit of detection is 200 ppm.

	HMC			Int HMC: (4-9.7 mole %, 1-2.5 wt% Mg)			LMC		
Fabric	# of analyses	Ave Sr (ppm)	Range Sr (ppm)	# of analyses	Ave Sr (ppm)	Range Sr (ppm)	# of analyses	Ave Sr (ppm)	Range Sr (ppm)
Calcite 1	195	1000	500-1550	5	760	330-1130	171	350	<200-990
Micro A	0	n/a	n/a	5	520	<200-770	47	300	<200-1100
Perm Anhedral	22	990	650-1410	0	n/a	n/a	55	320	<200-700
Radial Fibrous	19	700	470-940	6	600	480-600	28	430	<200-710
Micro B	2	680	530-830	1	660	660	5	250	<200-400
Clear Anhedral	0	n/a	n/a	0	n/a	n/a	5	210	<200-340
Totals	238	843		17	635		311	310	

VITA

Name: Courtney Page Jones

Address: Southwestern Energy Company
515 W. Greens Road
Houston, TX 77067

Education: B.S., Geology, Texas A&M University, 2010
M.S., Geology, Texas A&M University, 2012